

000 001 002 003 004 005 006 007 008 009 010 011 012 013 014 015 016 017 018 019 020 021 022 023 024 025 026 027 028 029 030 031 032 033 034 035 036 037 038 039 040 041 042 043 044 045 046 047 048 049 050 051 052 053 DUAL-FORECASTER: A MULTIMODAL TIME SERIES MODEL INTEGRATING TEXTUAL CUES VIA DUAL- SCALE ALIGNMENT

Anonymous authors

Paper under double-blind review

ABSTRACT

Time series forecasting plays a vital role for decision-making across a wide range of real-world domains, which has been extensively studied. Most existing single-modal time series models rely solely on numerical series, which suffer from the limitations imposed by insufficient information. Recent studies have revealed that multimodal models can address the core issue by integrating textual information. However, these models primarily employ coarse-grained meta information designed for the whole dataset (*e.g.*, task instruction, domain description, data statistics, etc.), while the use of sample-specific textual contexts remains underexplored. To this end, we propose Dual-Forecaster, a pioneering multimodal time series model that utilizes finer-grained textual information at the sample level through the well-designed dual-scale alignment technique. Specifically, we decouple the learning of semantic and patch-level features, enabling the direct extraction of both global semantic representations critical for cross-modal understanding and local patch features essential for time series forecasting. Our comprehensive evaluations demonstrate that Dual-Forecaster is a distinctly effective multimodal time series model that outperforms or is comparable to other state-of-the-art models, highlighting the superiority of integrating textual information for time series forecasting. This work opens new avenues in the integration of textual information with numerical time series data for multimodal time series analysis.

1 INTRODUCTION

With the massive accumulation of time series data in such diverse domains as retail (Leonard, 2001), electricity (Liu et al., 2023a), traffic (Shao et al., 2022), finance (Li et al., 2022), and healthcare (Kaushik et al., 2020), time series forecasting has become a key part of decision-making. To date, while extensive research has been dedicated to time series forecasting, resulting in a multitude of proposed methodologies (Hyndman et al., 2008; Nie et al., 2023; Liu et al., 2023b; Ansari et al., 2024; Zhou et al., 2023), they are predominantly confined to single-modal models that rely exclusively on numerical time series data. Recent studies have shown that simple linear models ((Zeng et al., 2023; Xu et al., 2023)) can often match or even surpass the performance of state-of-the-art (SOTA) complex models, suggesting that current single-modal approaches may be nearing a saturation point.

To improve the model’s forecasting performance, it is crucial to introduce supplementary information that is not present in time series data. For example, when forecasting future product sales, combining numerical historical sales data with external factors, such as product iteration plans, strategic sales initiatives, and unforeseeable events such as pandemics, enables us to give a sales forecast that aligns more closely with business expectations. This supplementary information typically appears in the form of unstructured text, which is rich in semantic details reflecting temporal causality and system dynamics. However, quantifying such valuable information into auxiliary time series data remains challenging, which presents a significant hurdle to its integration in enhancing the reliability of time series forecasting.

Recently, there has been a surge in research proposing multimodal time series models that integrate text as an auxiliary input modality (Liu et al., 2024b; Jin et al., 2024; Liu et al., 2024a; Xu

et al., 2024; Wang et al., 2025). This methodology effectively overcomes the intrinsic limitations of traditional time series forecasting methods, thereby significantly enhancing models' accuracy and effectiveness. However, in these works, the textual input consists of coarse-grained dataset-level information, such as task instructions and dataset descriptions, making it difficult to provide finer-grained sample-level discernibility. Moreover, these models focus on aligning patch-level time series features with text for time series forecasting while overlooking the significance of semantic-level features in enhancing multimodal understanding, which hinders their ability to capture complex connections between textual and time series data. Thus, it is necessary to develop an effective alignment technique tailored for finer-grained sample-level textual data to learn multimodal embeddings that will in turn enhance forecasting.

To tackle the aforementioned challenges, we introduce Dual-Forecaster, a cutting-edge time series forecasting model. Built upon a sophisticated framework, it effectively aligns finer-grained textual data at the sample level with time series data through the meticulous-designed dual-scale alignment technique. It should be noted that the word 'Dual' in Dual-Forecaster has two different levels of meaning. On the one hand, it represents that Dual-Forecaster is a multimodal time series model capable of concurrently processing both textual and time series data. On the other hand, it denotes the model's capacity to extract features at both the semantic and patch levels, enabling a hierarchical integration of high-level semantic insights and fine-grained local patterns. Specifically, Dual-Forecaster comprises the textual branch and the temporal branch. The textual branch is designed to parse textual data and extract valuable insights embedded within, while the temporal branch specializes in modeling time series dynamics. To generate high-quality embeddings for accurate forecasting, we jointly optimize two core tasks: multimodal comprehension and time series forecasting. Central to our design is the dual-scale alignment technique, which decouples the learning of semantic and patch-level features. This enables the model to directly extract (1) global semantic representations—critical for multimodal comprehension and regularized by the **Text-Time Series Contrastive Loss**—and (2) local patch features—essential for time series forecasting, derived through the **Modality Interaction Module**.

To prove the effectiveness of our model, we conduct extensive experiments on twelve multimodal time series datasets, which consist of six constructed datasets including a synthetic dataset and five captioned public datasets, and six existing multimodal datasets. Experimental results demonstrate that Dual-Forecaster achieves competitive or superior performance when compared to other SOTA models on all datasets. In addition, ablation studies emphasize that performance improvement is attributed to the supplementary information provided by the textual data.

Our main contributions in this work are threefold:

- (1) We propose a sophisticated framework for integrating textual and time series data, grounded in our dual-scale alignment technique. This framework is designed to generate time series embeddings enriched with semantic insights from text, thereby enabling Dual-Forecaster to achieve more robust forecasting performance.
- (2) We introduce Dual-Forecaster, a novel time series forecasting model that tackles the critical challenge of underutilized finer-grained textual signals in multimodal time series forecasting. By systematically integrating sample-specific textual semantics with temporal dynamics, our model enables the discerning of complex inter-variable dependencies.
- (3) Extensive experiments across multiple datasets validate that Dual-Forecaster achieves SOTA performance on time series forecasting task. Ablation studies further highlight the critical role of the dual-scale alignment technique, demonstrating its indispensable contribution to the model's superior performance.

2 RELATED WORK

Time series forecasting. Time series forecasting models can be roughly categorized into statistical models and deep learning models. Statistical models such as ETS, ARIMA (Hyndman et al., 2008) can be fitted to a single time series and used to make predictions of future observations. Deep learning models, ranging from the classical LSTM (Hochreiter, 1997), TCN (Bai et al., 2018), to recently popular transformer-based models (Nie et al., 2023; Zhou et al., 2022; Zhang & Yan, 2023; Liu et al., 2023b), are developed for capturing nonlinear, long-term temporal dependencies. Even

108 though excellent performance has been achieved on specific tasks, these models lack generalizability
 109 to diverse time series data.

110 To overcome the challenge, the development of pre-trained time series foundation models has
 111 emerged as a burgeoning area of research. In the past two years, several time series foundation
 112 models have been introduced (Ansari et al., 2024; Garza & Mergenthaler-Canseco, 2023; Rasul
 113 et al., 2023; Das et al., 2024; Woo et al., 2024). All of them are pre-trained transformer-based
 114 models trained on a large corpus of time series data with time-series-specific designs in terms of time
 115 features, time series tokenizers, distribution heads, and data augmentation, among others. These
 116 pre-trained time series foundation models can adapt to new datasets and tasks without extensive
 117 from-scratch retraining, demonstrating superior zero-shot forecasting capability. Furthermore, ben-
 118 efiting from the impressive capabilities of pattern recognition, reasoning and generalization of Large
 119 Language Models (LLMs), recent studies have further explored tailoring LLMs for time series data
 120 through techniques such as fine-tuning (Zhou et al., 2023; Xue & Salim, 2023; Gruver et al., 2024)
 121 and model reprogramming (Jin et al., 2024; Cao et al., 2024; Pan et al., 2024; Sun et al., 2023).
 122 However, existing time series forecasting models have encountered a plateau in performance due
 123 to limited information contained in time series data. There is an evident need for additional data
 124 beyond the scope of time series to further refine forecasts.

125 **Text-guided time series forecasting.** Some works have attempted to address the prevalent issue of
 126 information insufficiency in the manner of text-guided time series forecasting, which includes text
 127 as an auxiliary input modality. A line of work investigate how to use some declarative prompts (e.g.,
 128 date information, task instructions, domain expert knowledge, event description, etc.) enriching the
 129 input time series to guide LLM reasoning (Liu et al., 2024b; Jin et al., 2024; Wang et al., 2025; Liu
 130 et al., 2024c; Williams et al., 2024). These approaches fall into two categories: directly prompting
 131 LLM for time series forecasting or aligning text and time series within the language space to exploit
 132 the inference potential of the LLMs. However, they ignore the key role played by the local temporal
 133 features in time series forecasting.

134 An alternative text-guided time series forecasting approach is to process textual and time series data
 135 separately by using different models, and then merge the information of two modalities through a
 136 modality interaction module to yield enriched time series representations for time series forecasting
 137 (Liu et al., 2024a; 2025; Xu et al., 2024). Our method belongs to this category, however, there is
 138 limited relevant research on time series. Liu et al. (2024a) develops MM-TFSlib, which provides
 139 a convenient multimodal integration framework. It can independently model numerical and textual
 140 series using different time series forecasting models and LLMs, and then combine these outputs
 141 using a learnable linear weighting mechanism to produce the final predictions. Liu et al. (2025)
 142 presents an LLM-empowered framework via cross-modality alignment for multivariate time series
 143 forecasting. The cross-modality alignment module aggregates the time series and LLM branches
 144 based on channel-wise similarity retrieval to enhance forecasting. Distinct from these methods, we
 145 focus on investigating how to utilize finer-grained textual information at the sample level to assist in
 146 time series forecasting. Moreover, We recognize that features at different scales play unique roles in
 147 enabling multimodal time series forecasting models to achieve better multimodal understanding and
 148 more accurate time series forecasting. To this end, we propose Dual-Forecaster, which can jointly
 149 optimize semantic and patch-level features based on the dual-scale alignment technique to obtain
 150 time series representations with rich semantics, aiming to better enhance the model’s time series
 151 forecasting ability.

152 3 METHODOLOGY

153 3.1 PROBLEM FORMULATION

154 Given a dataset of N numerical time series and their corresponding textual series, $\mathcal{D} =$
 155 $\{(\mathbf{X}_{t-L:t}^{(i)}, \mathbf{X}_{t:t+h}^{(i)}, \mathbf{S}_{t-L:t}^{(i)})\}_{i=1}^N$, where $\mathbf{X}_{t-L:t}^{(i)}$ is the input variable of the numerical time series,
 156 L is the specified *look back window* length, and $\mathbf{X}_{t:t+h}^{(i)}$ is the ground truth of *horizon window*
 157 length h . $\mathbf{S}_{t-L:t}^{(i)}$ is the overall description of $\mathbf{X}_{t-L:t}^{(i)}$, which can be used to augment the model’s
 158 capacity to learn the relationships between different time series by combining detailed descrip-
 159 tive information about the time series. The goal is to maximize the log-likelihood of the pre-
 160

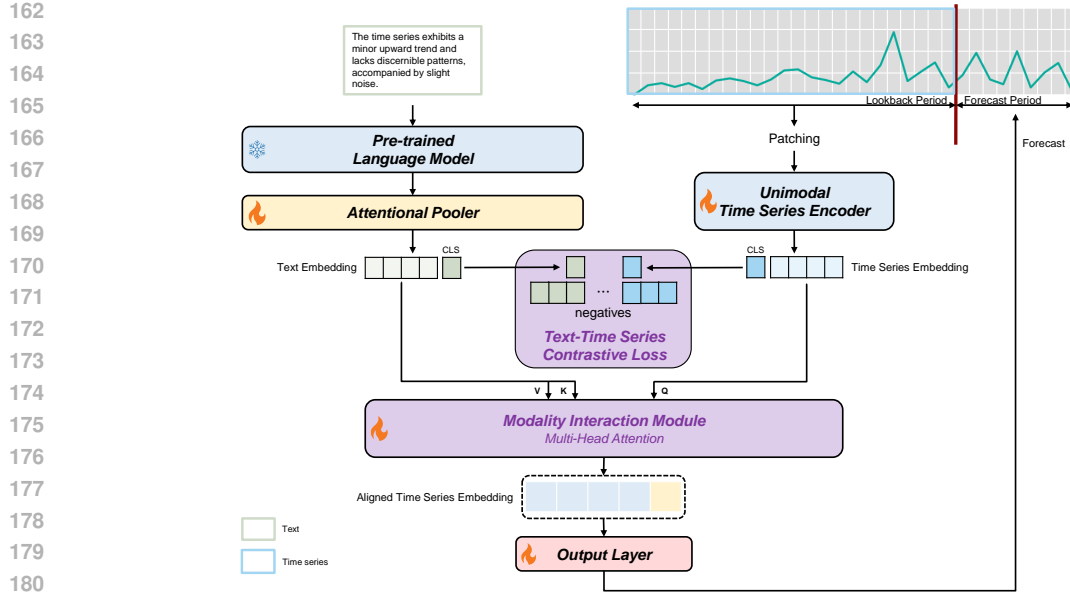


Figure 1: Overall architecture of Dual-Forecaster. Top left is the textual branch with text as input, and top right is the temporal branch with time series as input. Based on the obtained textual features and time series embeddings, to achieve effective alignment of semantic and patch-level features, we propose the **Dual-Scale Alignment** framework that employs the **Text-Time Series Contrastive Loss** and the **Modality Interaction Module**. The outputs of time series embeddings from the **Modality Interaction Module** are then projected through the Output Layer to generate the final forecasts.

dicted distribution $p(X_{t:t+h}|\hat{\phi})$ obtained from the distribution parameters $\hat{\phi}$ learned by the model $f_{\theta} : (X_{t-L:t}, S_{t-L:t}) \rightarrow \hat{\phi}$ based on historical time series data and its corresponding descriptive textual information.

$$\begin{aligned} & \max_{\theta} \mathbb{E}_{(X, S) \sim p(\mathcal{D})} \log p(X_{t:t+h}|\hat{\phi}) \\ & \text{s.t. } \hat{\phi} = f_{\theta} : (X_{t-L:t}, S_{t-L:t}) \end{aligned} \quad (1)$$

where $p(\mathcal{D})$ is the data distribution used for sampling numerical time series and their corresponding textual series.

3.2 ARCHITECTURE

Illustrated in Figure 1, our proposed Dual-Forecaster consists of two branches: the textual branch and the temporal branch. The textual branch comprises a pre-trained language model and an attentional pooler. The frozen pre-trained language model is responsible for tokenization, encoding, and embedding of text. The attentional pooler is adopted to customize textual representations produced by the language model into different scales for two core tasks of multimodal understanding and time series forecasting. The temporal branch consists of a unimodal time series encoder that is used for patching and embedding of time series. It is noteworthy that the [CLS] as a global representation of time series is introduced into the embedded representation vector. In concrete, the textual branch takes the historical text $S_{t-L:t}$ as input to obtain their corresponding embeddings $\tilde{S}_{q(t-L:t)}$, $\tilde{S}_{CLS(t-L:t)}$. The temporal branch works with the historical time series $X_{t-L:t}$ to obtain its corresponding embedding $\tilde{X}_{P(t-L:t)}$, $\tilde{X}_{CLS(t-L:t)}$. To achieve effective alignment of semantic-level features ($\tilde{S}_{CLS(t-L:t)}$, $\tilde{X}_{CLS(t-L:t)}$) and patch-level features ($\tilde{S}_{q(t-L:t)}$, $\tilde{X}_{P(t-L:t)}$), we implement the dual-scale alignment technique, which is composed of two key components: the text-time series contrastive loss and the modality interaction module. In the following section, we will provide a detailed explanation of these two components.

216 3.2.1 TEXT-TIME SERIES CONTRASTIVE LOSS
217

218 Previous multimodal time series models, whether they integrate historical texts like descriptions of
219 input time series (Liu et al., 2024a; 2025) or future texts such as news and channel descriptions
220 (Xu et al., 2024), typically utilize separate textual and temporal branches to process their respective
221 modality data. Subsequently, they employ a cross-attention-based modality interaction module to
222 facilitate the integration of these distinct modality data. Given that the textual features and time
223 series embeddings reside in their own high-dimensional spaces, it is challenging for these models to
224 effectively learn and model their interactions. While model reprogramming techniques like Time-
225 LLM (Jin et al., 2024) align time series representations into the language space, thus unleashing the
226 potential of LLM as a predictor, these approaches often overlook the critical role of local temporal
227 features.

228 Inspired by the VLP framework in CV (Li et al., 2021; Yu et al., 2022), in this work, we attempt
229 to align textual features and time series embeddings into the unified high-dimensional space before
230 fusing in the modality interaction modules. Therefore, we develop the text-time series contrastive
231 loss to deal with this problem. Specifically, for each input time series $X_{t-L:t}^{(i)} \in \mathbb{R}^{1 \times L}$, it is first
232 normalized to have zero mean and unit standard deviation in mitigating the time series distribution
233 shift. Then, we divide it into P consecutive non-overlapping patches with length L_p . Given these
234 patches $X_{P(t-L:t)}^{(i)} \in \mathbb{R}^{P \times L_p}$, we adopt a simple linear layer to embed them as $\hat{X}_{P(t-L:t)}^{(i)} \in \mathbb{R}^{P \times d_m}$,
235 where d_m is the dimensions of time series features. On this basis, we introduce the time series CLS
236 token $\hat{X}_{CLS(t-L:t)}^{(i)} \in \mathbb{R}^{1 \times d_m}$. Let $\hat{X}_{t-L:t}^{(i)} = [\hat{X}_{P(t-L:t)}^{(i)} \hat{X}_{CLS(t-L:t)}^{(i)}] \in \mathbb{R}^{(P+1) \times d_m}$. We use
237 the n_{uni} unimodal time series encoder layers containing *Multi-Head Self-Attention (MHSA)* layers
238 to process time series, and finally take the outputs of the n_{uni}^{th} layer as the embeddings $\tilde{X}_{t-L:t}^{(i)} \in \mathbb{R}^{(P+1) \times d_m}$:
239

$$240 \tilde{X}_{t-L:t}^{(i)} = \left(MHSA \left(\hat{X}_{t-L:t}^{(i)} \right) + \hat{X}_{t-L:t}^{(i)} \right)_{n_{uni}^{th}} = \left[\tilde{X}_{P(t-L:t)}^{(i)} \tilde{X}_{CLS(t-L:t)}^{(i)} \right] \quad (2)$$

241 For each historical text $S_{t-L:t}^{(i)}$, we use the pre-trained language model for tokenization, encoding,
242 and embedding to obtain $\hat{S}_{G(t-L:t)}^{(i)} \in \mathbb{R}^{G \times d}$, where G represents the number of tokens encoded in
243 the historical text and d is the dimensions of textual features. On this basis, we introduce learnable
244 text query $\hat{Q}_q^{(i)} \in \mathbb{R}^{q \times d_m}$ and text CLS token $\hat{Q}_{CLS}^{(i)} \in \mathbb{R}^{1 \times d_m}$. Let $\hat{Q}^{(i)} = [\hat{Q}_q^{(i)} \hat{Q}_{CLS}^{(i)}] \in \mathbb{R}^{(q+1) \times d_m}$. We use a *Multi-Head Cross-Attention (MHCA)* layer with $\hat{Q}^{(i)}$ as query and $\hat{S}_{G(t-L:t)}^{(i)}$
245 as key and value to obtain the embedding $\tilde{S}_{t-L:t}^{(i)} \in \mathbb{R}^{(q+1) \times d_m}$:
246

$$247 \tilde{S}_{t-L:t}^{(i)} = MHCA \left(\hat{Q}^{(i)}, \hat{S}_{G(t-L:t)}^{(i)} \right) = \left[\tilde{S}_{q(t-L:t)}^{(i)} \tilde{S}_{CLS(t-L:t)}^{(i)} \right] \quad (3)$$

248 Given the outputs of $\tilde{S}_{CLS(t-L:t)}^{(i)}$ and $\tilde{X}_{CLS(t-L:t)}^{(i)}$ from the textual branch and the temporal branch,
249 respectively, the text-time series contrastive loss is defined as:

$$250 \sim_i = \tilde{X}_{CLS(t-L:t)}^{(i)} \odot \tilde{S}_{CLS(t-L:t)}^{(i)}$$

$$251 \mathcal{L}_{contrastive} = -\frac{1}{B} \left(\sum_i^B \log \frac{\exp(\sim_i^T y_i / \tau)}{\sum_{j=1}^B \exp(\sim_j^T y_j)} + \sum_i^B \log \frac{\exp(y_i^T \sim_i / \tau)}{\sum_{j=1}^B \exp(y_j^T \sim_j)} \right) \quad (4)$$

252 where B is the batch size, $y_i \in \mathbb{R}^{B \times B}$ is the one-hot label matrix from ground truth text-time series
253 pair label, and τ is the temperature to scale the logits.

254 3.2.2 MODALITY INTERACTION MODULE
255

256 To ensure effective alignment of distributions between historical textual and time series data, we use
257 the n_{mul} multimodal layers, including a *MHSA* operation and a *MHCA* operation in each layer, as the

270 modality interaction module to obtain the aligned time series embedding that integrates historical
 271 textual information. Formally, given $\tilde{\mathbf{S}}_{q(t-L:t)}^{(i)}$ and $\tilde{\mathbf{X}}_{P(t-L:t)}^{(i)}$ produced by the textual branch and
 272 the temporal branch, at each layer of the modality interaction module, we sequentially process and
 273 aggregate the textual and temporal information based on the *MHSA* and *MHCA* mechanism, and
 274 finally take the outputs of the n_{mul}^{th} layer as the aligned time series embeddings $\bar{\mathbf{X}}_{align}^{(i)} \in \mathbb{R}^{P \times d_m}$:
 275

$$\bar{\mathbf{X}}_{align}^{(i)} = \left(MHCA \left(MHSA \left(\tilde{\mathbf{X}}_{P(t-L:t)}^{(i)} \right) + \tilde{\mathbf{X}}_{P(t-L:t)}^{(i)}, \tilde{\mathbf{S}}_{q(t-L:t)}^{(i)} \right) + \tilde{\mathbf{X}}_{P(t-L:t)}^{(i)} \right)_{n_{mul}^{th}} \quad (5)$$

279 3.2.3 OUTPUT LAYER

280 To maintain homogeneity with $\mathcal{L}_{contrastive}$, we use negative log-likelihood loss as the forecast loss,
 281 which constrains the model’s predicted distribution to closely align with the actual distribution.
 282 Specifically, given $\bar{\mathbf{X}}_{align}^{(i)}$, we linearly project the last token embedding $\bar{\mathbf{X}}_{align}^{(i)} \in \mathbb{R}^{1 \times d_m}$ to
 283 obtain the distribution parameters of the Student’s T-distribution prediction head. The forecast loss
 284 used is defined as:
 285

$$\mathcal{L}_{forecast} = -\frac{1}{B} \sum_i^B \log p \left(\mathbf{X}_{t:t+h}^{(i)} | \hat{\phi} \left(\bar{\mathbf{X}}_{align}^{(i)}[-1] \right) \right) \quad (6)$$

286 The overall loss during training is the summation of the forecast loss $\mathcal{L}_{forecast}$ and the contrastive
 287 loss $\mathcal{L}_{contrastive}$ as follows:
 288

$$\mathcal{L} = \mathcal{L}_{forecast} + \mathcal{L}_{contrastive} \quad (7)$$

293 4 MAIN RESULTS

294 **Datasets.** To demonstrate the effectiveness of the proposed Dual-Forecaster, we employ three
 295 types of dataset—synthetic dataset, captioned-public dataset, and existing multimodal time series
 296 dataset—encompassing a spectrum of difficulty levels from simple to complex. These three dataset
 297 categories exhibit different degrees of authenticity: synthetic dataset consists of synthetic time
 298 series-text pairs; captioned-public dataset contains real time series data with corresponding syn-
 299 thetic text annotations, and existing multimodal time series dataset are more reflective of real-world
 300 scenarios. Leveraging these datasets enables a systematic, stepwise validation of the practical ef-
 301 fectiveness of the Dual-Forecaster. We firstly design six multimodal time series benchmark datasets
 302 across two categories: synthetic dataset and captioned-public dataset. Additionally, we gather six
 303 existing multimodal time series benchmark datasets from the Time-MMD dataset. The Time-MMD
 304 dataset (Liu et al., 2024a) encompasses such nine primary data domains as climate, health, energy,
 305 and traffic. It is the first high-quality and multi-domain, multimodal time series dataset, providing
 306 great convenience for verifying the model’s multimodal time series forecasting ability in real-world
 307 scenarios. We conduct extensive experiments on them and compare Dual-Forecaster against a col-
 308 lection of representative methods from the recent time series forecasting landscape, our approach
 309 displays competitive or stronger results in multiple benchmarks.
 310

311 **Baseline Models.** We carefully select 11 forecasting methods as our baselines which fall into two
 312 categories: *single-modal models* and *multimodal models*. For the *single-modal models*, they include
 313 DLinear (Zeng et al., 2023), FITS (Xu et al., 2023), PatchTST (Nie et al., 2023), iTransformer
 314 (Liu et al., 2023b), and Chronos (Ansari et al., 2024). For the *Multimodal models*, they consist of
 315 GPT4TS (Zhou et al., 2023), UniTime (Liu et al., 2024b), Time-LLM (Jin et al., 2024), MM-TSFlib
 316 (Liu et al., 2024a), TimeCMA (Liu et al., 2025) and ChatTime (Wang et al., 2025). It is worth noting
 317 that we employ GPT2 as LLM backbone and iTransformer as time series forecasting backbone
 318 for the MM-TSFlib model based on the experimental results reported in the original paper. We
 319 contrast Dual-Forecaster with the *single-modal models* to illustrate how textual insights can enhance
 320 forecasting performance. Comparisons with the *multimodal models* highlight the advancement of
 321 Dual-Forecaster’s dual-scale alignment technique in cross-modality alignment, demonstrating its
 322 superiority over direct prompting and simple multimodal fusion methods, which in turn can further
 323 elevate the model’s forecasting performance. Note that all these methods train a dedicated model
 324 for each evaluated dataset except for two foundation models of Chronos and ChatTime, which are
 325 directly used for inference.

324

325 Table 1: Forecasting result on synthetic dataset. The best and second best results are in **bold** and
326 underlined.

Methods	Dual-Forecaster		GPT4TS		UniTime		Time-LLM		MM-TSFlib		TimeCMA		ChatTime		Chronos		DLlinear		FITS		PatchTST		iTransformer		
Metric	MSE	MAE	MSE	MAE	MSE	MAE	MSE	MAE	MSE	MAE	MSE	MAE	MSE	MAE	MSE	MAE	MSE	MAE	MSE	MAE	MSE	MAE	MSE	MAE	
synthetic dataset	30	0.5970	<u>0.5224</u>	0.9467	0.7139	0.6684	0.5911	0.8907	0.6976	<u>0.6013</u>	0.5419	3.0644	1.4267	1.1251	0.7111	0.9273	0.6326	1.2190	0.8139	2.7585	1.3254	0.6015	<u>0.5394</u>	0.6190	0.5529

327

328

329

330

331 Table 2: Forecasting result on captioned-public datasets. The best result is highlighted in **bold** and
332 underlined.

Methods	Dual-Forecaster		GPT4TS		UniTime		Time-LLM		MM-TSFlib		TimeCMA		ChatTime		Chronos		DLlinear		FITS		PatchTST		iTransformer		
Metric	MSE	MAE	MSE	MAE	MSE	MAE	MSE	MAE	MSE	MAE	MSE	MAE	MSE	MAE	MSE	MAE	MSE	MAE	MSE	MAE	MSE	MAE	MSE	MAE	
ETTm1	96	1.3203	<u>0.8061</u>	1.4641	0.8787	1.4034	0.8607	1.4457	0.8730	1.3626	0.8426	2.4790	1.2475	1.7347	0.9613	1.5638	0.8987	1.5601	0.9198	2.2858	1.1810	1.4544	0.8619	<u>1.3393</u>	<u>0.8299</u>
ETTm2	96	0.9363	<u>0.6108</u>	1.1184	0.7042	1.0397	0.6752	1.1199	0.7054	1.0325	0.6691	2.0336	1.0727	1.8680	0.9642	1.6991	0.8582	1.1663	0.7332	1.7418	0.9709	0.9419	<u>0.6280</u>	1.0210	0.6557
ETTh1	96	<u>1.3935</u>	0.9017	1.5078	0.9495	<u>1.4647</u>	<u>0.9178</u>	1.5919	0.9914	1.4967	0.9347	1.6117	1.0065	1.9604	1.0821	1.5282	0.9402	1.4999	0.9505	1.6004	0.9952	1.6009	0.9603	1.5128	0.9438
ETTh2	96	0.9429	<u>0.7467</u>	<u>0.9612</u>	0.7679	1.0028	0.7820	1.0586	0.8083	0.9616	<u>0.7644</u>	1.4177	0.9220	1.5014	0.9530	1.0474	0.7761	0.9951	0.7847	1.2858	0.8875	1.0349	0.7879	0.9803	0.7703
exchange-rate	96	<u>2.2011</u>	0.8458	3.0947	1.1203	2.5676	0.9933	3.0564	1.1111	2.6365	1.0061	4.4906	1.4850	2.3079	1.0291	2.7269	<u>0.9773</u>	3.1668	1.1146	4.4656	1.4831	<u>2.2656</u>	1.0016	2.6426	0.9977

337

338

339

340 **Implementation Details.** We utilize a six-layers pre-trained *RoBERTa* (Liu, 2019) model to pro-
341 cess text inputs. All experiments are repeated three times. All computations are performed on a
342 single NVIDIA GeForce RTX 4070 Ti GPU.

343

344

4.1 EVALUATION ON SYNTHETIC DATASET

345

346

347 **Setups.** The synthetic dataset is adopted to assess the model’s capacity to utilize textual infor-
348 mation for time series forecasting while effectively mitigating distribution drift. It is composed of
349 simulated time series data containing different proportions of trend, seasonality, noise components,
350 and switch states. For a fair comparison, the input time series *look back window* length L is set as
351 200, and the prediction horizon h is set as 30. Consistent with prior works, we choose the Mean
352 Square Error (MSE) and Mean Absolute Error (MAE) as the default evaluation metrics.

353

354 **Results.** Table 1 presents the performance comparison of various models on synthetic dataset. Our
355 model consistently outperforms all baseline models.

356

4.2 EVALUATION ON CAPTIONED-PUBLIC DATASETS

357

358 **Setups.** The captioned-public datasets are utilized to evaluate the model’s capability of better
359 performing time series forecasting by combining textual information to eliminate uncertainty in
360 complex time series scenarios. They consist of the captioned version of ETTm1, ETTm2, ETTh1,
361 ETTh2, and exchange-rate datasets which have been extensively adopted for benchmarking various
362 time series forecasting models. In this case, the input time series *look back window* length L is set to
363 336, and the prediction horizon h is fixed as 96. It should be noted that due to resource constraints,
364 we construct relatively small datasets on the basis of these datasets by setting the value of stride and
365 conduct experiments on them. For ETTm1 and ETTm2 datasets, stride is set to 16, while for ETTh1
366 and ETTh2 datasets, stride is fixed as 4. For exchange-rate datasets, stride is set to 12.

367

368 **Results.** As demonstrated in Table 2, Dual-Forecaster consistently surpasses all baselines by a
369 large margin, over **2.3%/4.6%** w.r.t. the second-best in MSE/MAE reduction.

370

4.3 EVALUATION ON EXISTING MULTIMODAL TIME SERIES DATASETS

371

372 **Setups.** With the increasing availability of multimodal time series datasets, we have assembled
373 a collection of existing datasets to further validate the Dual-Forecaster’s real-world applicability.
374 These datasets from the Time-MMD datasets feature more general textual data, such as reports and
375 news, rather than time series shape-based descriptions. Moreover, the textual data in these datasets
376 contains varying degrees of inaccuracies, which is more in line with the real-world scenarios.

377

378 **Results.** As demonstrated in Table 3, Dual-Forecaster consistently outperforms all baselines by a
379 significant margin, achieving a **12.5%** reduction in MSE compared to the second-best model. This
380 underscores the actual effectiveness of Dual-Forecaster in real-world forecasting scenarios.

378

379
Table 3: Forecasting result on existing multimodal time series datasets. The best result is highlighted
380 in **bold** and the second best is highlighted in underlined.
381

Methods	Dual-Forecaster		GPT4TS		UniTime		Time-LLM		MM-TSFlit		TimeCMA		ChatTime		Chronos		DLiner		FTTS		PatchTST		iTTransformer		
Metric	MSE	MAE	MSE	MAE	MSE	MAE	MSE	MAE	MSE	MAE	MSE	MAE	MSE	MAE	MSE	MAE	MSE	MAE	MSE	MAE	MSE	MAE	MSE	MAE	
Time-MMD-Climate	8	0.8520	<u>0.7496</u>	1.4222	0.9604	1.2687	0.8827	1.3398	0.9217	1.1386	0.8212	1.3713	0.9444	1.5118	0.9420	<u>1.0346</u>	0.8365	2.9057	1.4165	1.5494	0.9776	1.0975	0.8054	1.1392	0.8194
Time-MMD-Economy	8	<u>0.7785</u>	0.3366	0.2350	0.3902	0.2691	0.4116	0.2330	0.3858	0.2066	0.3583	0.2234	0.3708	0.3199	0.4491	0.2782	0.4229	8.6163	2.5406	0.2766	0.4184	<u>0.1960</u>	0.3512	0.1963	0.3493
Time-MMD-SocialGood	8	1.2364	<u>0.6978</u>	1.5420	0.6398	1.8239	0.6488	<u>1.5172</u>	0.6106	1.8615	0.5550	1.5433	0.6142	1.6290	0.6176	1.5912	0.6228	4.3273	1.8199	1.7227	0.6789	1.7589	0.5761	1.7128	0.5329
Time-MMD-Traffic	8	0.1814	0.2984	0.2763	0.3953	0.3127	0.4043	0.2299	0.3370	0.1892	<u>0.2491</u>	0.2805	0.3971	0.4648	0.5312	0.3920	0.4944	4.3517	1.8561	0.3542	0.4570	<u>0.1828</u>	0.2591	0.1917	0.2503
Time-MMD-Energy	12	0.0853	<u>0.2015</u>	0.2069	0.3445	0.1158	0.2527	0.1263	0.2619	0.1146	0.2472	0.2553	0.3872	0.0851	0.4971	0.1199	0.2297	1.2669	0.8204	0.2893	0.4086	<u>0.1031</u>	0.2217	0.1123	0.2415
Time-MMD-Health-US	12	0.8563	<u>0.5931</u>	1.5428	0.8597	1.0753	0.7117	1.1728	0.7331	<u>0.9710</u>	0.6308	2.0369	1.0064	1.5114	0.8102	1.5394	0.7680	2.2140	1.0484	2.2509	1.1193	1.1000	0.7233	1.0467	0.6573

382
383
384
385
386
387
388 4.4 MODEL ANALYSIS
389

390 **Cross-modality Alignment.** To better illustrate the effectiveness of the model design in Dual-
391 Forecaster, we construct four model variants and conduct ablation experiments on synthetic dataset
392 and ETTm2 dataset. The experimental results presented in Table 4 demonstrate the importance
393 of integrating textual information for time series forecasting to achieve optimal performance, and
394 also validate the soundness of the design of the dual-scale alignment techniques. Employing tex-
395 tual information results in MSE/MAE of **0.5970/0.5224** (versus 0.6135/0.5379) on synthetic dataset
396 and **0.9363/0.6108** (versus 0.9507/0.6060) on ETTm2, respectively. Without Modality Interaction
397 Module, we observe an average performance degradation of **0.7%**, while the average performance
398 reduction becomes more obvious (**1.4%**) in the absence of Text-Time Series Contrastive Loss. Ex-
399 perimental results demonstrate that as the two components of the dual-scale alignment technique,
400 Text-Time Series Contrastive Loss and Modality Interaction Module are both critical for deriving
401 high-quality and semantically rich time series representations. Notably, the absence of the Text-Time
402 Series Contrastive Loss leads to more significant performance degradation in metrics. We attribute
403 this to Text-Time Series Contrastive Loss’s discernibility at the sample level, which enables it to ef-
404 fectively capture inter-variable relationships and reflect them in the final time series representations.
405

406
407 Table 4: Ablation on synthetic dataset and ETTm2 with prediction horizon 30 and 96, respectively.
The best results are highlighted in **bold**.
408

Model Variants	synthetic dataset		ETTm2	
	MSE	MAE	MSE	MAE
Dual-Forecaster	0.5970	0.5224	0.9363	0.6108
w/o Texts	0.6135	0.5379	0.9507	0.6060
w/ Texts				
→ w/o Text-Time Series Contrastive Loss	0.6057	0.5315	0.9571	0.6117
→ w/o Modality Interaction Module	0.6038	0.5254	0.9480	0.6102

416
417 **Cross-modality Alignment Interpretation.** We present a case study on synthetic dataset, as illus-
418 trated in Figure 2, to demonstrate the alignment effect between text and time series. This is achieved
419 by displaying the similarity matrix that captures the relationship between text features and time se-
420 ries embeddings. The time series data is visualized above the matrix, while its corresponding text
421 descriptions are on the left. For example, the 6th subplot depicts a sequence with an exponential up-
422 ward trend over time, corresponding to the text description ”exponential upward trend”. Our model
423 accurately establishes the correlation between text and time series, as evidenced by the high simi-
424 larity between their representations (the value at the 6th row and 6th column of the similarity matrix is
425 0.94). Additionally, the text description enables the establishment of varying degrees of associations
426 between different variables. For instance, the similar upward trends in the 6th subplot and the 1st/4th
427 subplots are manifested as values of 0.41 and 0.42 at the 6th row and 1st/4th columns in the simi-
428 larity matrix, respectively. In contrast, less relevant variables show low values in the similarity matrix.
429 This result shows that Dual-Forecaster is capable of autonomously discern potential connections
430 between text and time series except be able to accurately recognize the genuine pairing text-time
431 series relationships. This indicates that our model possesses advanced multimodal comprehension
432 capability, which has a positive influence on improving the model’s forecasting performance.

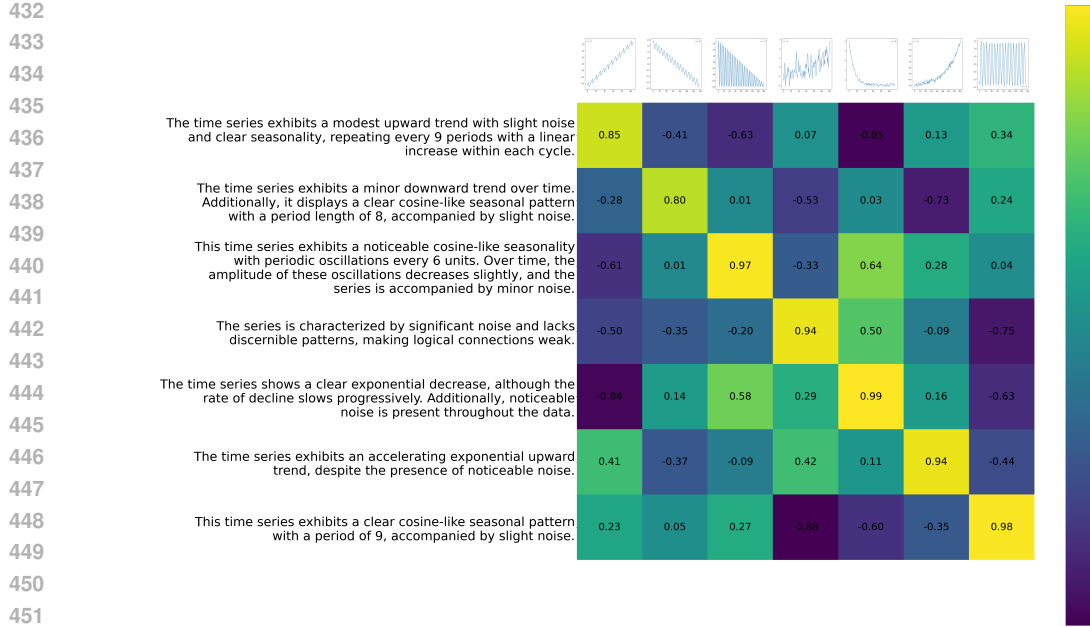


Figure 2: A showcase of text-time series alignment. The values in the matrix represent the similarity between the high-dimensional representation of the time series (above the matrix) and the corresponding textual description (on the left side of the matrix). The higher the similarity, the better the match between the time series and the text.

Cross-modality Alignment Efficiency Table 5 provides an overall efficiency analysis of Dual-Forecaster with and without cross-modal alignment techniques. Our model’s unimodal time series encoder is lightweight, and the overall efficiency of Dual-Forecaster is actually capped by the leveraged effective cross-modal alignment module. This is favorable in balancing forecasting performance and efficiency.

5 CONCLUSION

In this work, we present Dual-Forecaster, an innovative multimodal time series model that integrates sample-specific textual semantics with temporal dynamic to generate more accurate and reasonable forecasts. Our model capitalizes on the meticulously-designed dual-scale alignment technique comprising the text-time series contrastive loss and modality interaction module. This technique is designed to concurrently extract semantic and patch-level features, which are crucial for cross-modal understanding and time series forecasting, respectively. We conduct extensive experiments on twelve datasets to demonstrate the effectiveness of Dual-Forecaster and highlight the superiority of incorporating textual data for time series forecasting.

Limitations & Future Work While Dual-Forecaster has achieved remarkable performance in text-guided time series forecasting, there remains room for further improvements. Due to resource constraints, a comprehensive hyperparameter tuning was not performed, suggesting that the reported results of Dual-Forecaster may be sub-optimal. In terms of multimodal time series dataset, the lack of a standardized and efficient annotation methodology often leads to inadequate annotation quality on real-world datasets, with the issue being particularly pronounced in the annotation of long time series. Future work should focus on developing a more elegant time series annotator, leveraging the text-time series alignment techniques that are fundamental to Dual-Forecaster. In terms of downstream task, further research should explore the potential of expanding Dual-Forecaster to encompass a broad spectrum of multimodal time series analysis capabilities.

486 REFERENCES
487

488 Abdul Fatir Ansari, Lorenzo Stella, Caner Turkmen, Xiyuan Zhang, Pedro Mercado, Huibin Shen,
489 Oleksandr Shchur, Syama Syndar Rangapuram, Sebastian Pineda Arango, Shubham Kapoor,
490 Jasper Zschiegner, Danielle C. Maddix, Michael W. Mahoney, Kari Torkkola, Andrew Gor-
491 don Wilson, Michael Bohlke-Schneider, and Yuyang Wang. Chronos: Learning the language
492 of time series. *Transactions on Machine Learning Research*, 2024. ISSN 2835-8856. URL
493 <https://openreview.net/forum?id=gerNCVqqtR>.

494 Shaojie Bai, J Zico Kolter, and Vladlen Koltun. An empirical evaluation of generic convolutional
495 and recurrent networks for sequence modeling. *arXiv preprint arXiv:1803.01271*, 2018.

496 Defu Cao, Furong Jia, Sercan O Arik, Tomas Pfister, Yixiang Zheng, Wen Ye, and Yan Liu. TEMPO:
497 Prompt-based generative pre-trained transformer for time series forecasting. In *The Twelfth In-
498 ternational Conference on Learning Representations*, 2024. URL [https://openreview.
499 net/forum?id=YH5w120UuU](https://openreview.net/forum?id=YH5w120UuU).

500 Abhimanyu Das, Weihao Kong, Rajat Sen, and Yichen Zhou. A decoder-only foundation model for
501 time-series forecasting. In *Forty-first International Conference on Machine Learning*, 2024.

502 David H. Douglas and Thomas K. Peucker. Algorithms for the reduction of the number of points
503 required to represent a digitized line or its caricature. *Cartographica: The International Journal
504 for Geographic Information and Geovisualization*, 10:112–122, 1973. URL <https://api.semanticscholar.org/CorpusID:60447873>.

505 Azul Garza and Max Mergenthaler-Canseco. Timegpt-1, 2023.

506 Nate Gruver, Marc Finzi, Shikai Qiu, and Andrew G Wilson. Large language models are zero-shot
507 time series forecasters. *Advances in Neural Information Processing Systems*, 36, 2024.

508 S Hochreiter. Long short-term memory. *Neural Computation MIT-Press*, 1997.

509 Rob Hyndman, Anne B Koehler, J Keith Ord, and Ralph D Snyder. *Forecasting with exponential
510 smoothing: the state space approach*. Springer Science & Business Media, 2008.

511 Ming Jin, Shiyu Wang, Lintao Ma, Zhixuan Chu, James Y Zhang, Xiaoming Shi, Pin-Yu Chen, Yux-
512 uan Liang, Yuan-Fang Li, Shirui Pan, and Qingsong Wen. Time-LLM: Time series forecasting by
513 reprogramming large language models. In *International Conference on Learning Representations
514 (ICLR)*, 2024.

515 Shruti Kaushik, Abhinav Choudhury, Pankaj Kumar Sheron, Nataraj Dasgupta, Sayee Natarajan,
516 Larry A Pickett, and Varun Dutt. Ai in healthcare: time-series forecasting using statistical, neural,
517 and ensemble architectures. *Frontiers in big data*, 3:4, 2020.

518 Diederik P Kingma. Adam: A method for stochastic optimization. *arXiv preprint arXiv:1412.6980*,
519 2014.

520 Michael Leonard. Promotional analysis and forecasting for demand planning: a practical time series
521 approach. *with exhibits*, 1, 2001.

522 Junnan Li, Ramprasaath Selvaraju, Akhilesh Gotmare, Shafiq Joty, Caiming Xiong, and Steven
523 Chu Hong Hoi. Align before fuse: Vision and language representation learning with momentum
524 distillation. *Advances in neural information processing systems*, 34:9694–9705, 2021.

525 Na Li, Donald M Arnold, Douglas G Down, Rebecca Barty, John Blake, Fei Chiang, Tom Courtney,
526 Marianne Waito, Rick Trifunov, and Nancy M Heddle. From demand forecasting to inventory
527 ordering decisions for red blood cells through integrating machine learning, statistical modeling,
528 and inventory optimization. *Transfusion*, 62(1):87–99, 2022.

529 Chenxi Liu, Qianxiong Xu, Hao Miao, Sun Yang, Lingzheng Zhang, Cheng Long, Ziyue Li, and
530 Rui Zhao. TimeCMA: Towards llm-empowered multivariate time series forecasting via cross-
531 modality alignment. In *AAAI*, 2025.

540 Haoxin Liu, Shangqing Xu, Zhiyuan Zhao, Lingkai Kong, Harshavardhan Kamarthi, Aditya B.
 541 Sasanur, Megha Sharma, Jiaming Cui, Qingsong Wen, Chao Zhang, and B. Aditya Prakash.
 542 Time-mmd: Multi-domain multimodal dataset for time series analysis. In A. Globerson,
 543 L. Mackey, D. Belgrave, A. Fan, U. Paquet, J. Tomczak, and C. Zhang (eds.), *Advances in Neural*
 544 *Information Processing Systems*, volume 37, pp. 77888–77933. Curran Associates, Inc., 2024a.
 545 URL https://proceedings.neurips.cc/paper_files/paper/2024/file/8e7768122f3eec6d77cd2b424b72413-Paper-Datasets_and_Benchmarks_Track.pdf.

548 Hengbo Liu, Ziqing Ma, Linxiao Yang, Tian Zhou, Rui Xia, Yi Wang, Qingsong Wen, and Liang
 549 Sun. Sadi: A self-adaptive decomposed interpretable framework for electric load forecasting
 550 under extreme events. In *ICASSP 2023-2023 IEEE International Conference on Acoustics, Speech*
 551 *and Signal Processing (ICASSP)*, pp. 1–5. IEEE, 2023a.

552 Xu Liu, Junfeng Hu, Yuan Li, Shizhe Diao, Yuxuan Liang, Bryan Hooi, and Roger Zimmermann.
 553 Unitime: A language-empowered unified model for cross-domain time series forecasting. In
 554 *Proceedings of the ACM on Web Conference 2024*, pp. 4095–4106, 2024b.

556 Yinhan Liu. Roberta: A robustly optimized bert pretraining approach. *arXiv preprint*
 557 *arXiv:1907.11692*, 2019.

559 Yong Liu, Tengge Hu, Haoran Zhang, Haixu Wu, Shiyu Wang, Lintao Ma, and Mingsheng Long.
 560 itransformer: Inverted transformers are effective for time series forecasting. *arXiv preprint*
 561 *arXiv:2310.06625*, 2023b.

563 Yong Liu, Guo Qin, Xiangdong Huang, Jianmin Wang, and Mingsheng Long. Autotimes: Au-
 564 toregressive time series forecasters via large language models. In A. Globerson, L. Mackey,
 565 D. Belgrave, A. Fan, U. Paquet, J. Tomczak, and C. Zhang (eds.), *Advances in Neural*
 566 *Information Processing Systems*, volume 37, pp. 122154–122184. Curran Associates, Inc.,
 567 2024c. URL https://proceedings.neurips.cc/paper_files/paper/2024/file/dcf88cbc8d01ce7309b83d0ebaeb9d29-Paper-Conference.pdf.

569 Yuqi Nie, Nam H. Nguyen, Phanwadee Sinthong, and Jayant Kalagnanam. A time series is worth
 570 64 words: Long-term forecasting with transformers. In *International Conference on Learning*
 571 *Representations*, 2023.

573 Zijie Pan, Yushan Jiang, Sahil Garg, Anderson Schneider, Yuriy Nevmyvaka, and Dongjin Song.
 574 s^2 ip-llm: Semantic space informed prompt learning with llm for time series forecasting. In
 575 *Forty-first International Conference on Machine Learning*, 2024.

576 Adam Paszke, Sam Gross, Francisco Massa, Adam Lerer, James Bradbury, Gregory Chanan, Trevor
 577 Killeen, Zeming Lin, Natalia Gimelshein, Luca Antiga, et al. Pytorch: An imperative style, high-
 578 performance deep learning library. *Advances in neural information processing systems*, 32, 2019.

580 Kashif Rasul, Arjun Ashok, Andrew Robert Williams, Arian Khorasani, George Adamopoulos,
 581 Rishika Bhagwatkar, Marin Biloš, Hena Ghonia, Nadhir Hassen, Anderson Schneider, et al. Lag-
 582 llama: Towards foundation models for time series forecasting. In *R0-FoMo: Robustness of Few-
 583 shot and Zero-shot Learning in Large Foundation Models*, 2023.

585 Zezhi Shao, Zhao Zhang, Wei Wei, Fei Wang, Yongjun Xu, Xin Cao, and Christian S. Jensen.
 586 Decoupled dynamic spatial-temporal graph neural network for traffic forecasting. *Proc. VLDB*
 587 *Endow.*, 15(11):2733–2746, 2022.

588 Chenxi Sun, Hongyan Li, Yaliang Li, and Shenda Hong. Test: Text prototype aligned embedding to
 589 activate llm’s ability for time series. *arXiv preprint arXiv:2308.08241*, 2023.

591 Chengsen Wang, Qi Qi, Jingyu Wang, Haifeng Sun, Zirui Zhuang, Jinming Wu, Lei Zhang, and
 592 Jianxin Liao. Chattime: A unified multimodal time series foundation model bridging numerical
 593 and textual data. In *Proceedings of the AAAI Conference on Artificial Intelligence*, volume 39,
 pp. 12694–12702, 2025.

594 Andrew Robert Williams, Arjun Ashok, Étienne Marcotte, Valentina Zantedeschi, Jithendaraa Sub-
 595 ramanian, Roland Riachi, James Requeima, Alexandre Lacoste, Irina Rish, Nicolas Chapados,
 596 et al. Context is key: A benchmark for forecasting with essential textual information. *arXiv*
 597 *preprint arXiv:2410.18959*, 2024.

598 Gerald Woo, Chenghao Liu, Akshat Kumar, Caiming Xiong, Silvio Savarese, and Doyen Sahoo.
 599 Unified training of universal time series forecasting transformers. In *Forty-first International*
 600 *Conference on Machine Learning*, 2024.

601

602 Zhijian Xu, Ailing Zeng, and Qiang Xu. Fits: Modeling time series with $10k$ parameters. *arXiv*
 603 *preprint arXiv:2307.03756*, 2023.

604

605 Zhijian Xu, Yuxuan Bian, Jianyuan Zhong, Xiangyu Wen, and Qiang Xu. Beyond trend and pe-
 606 riodicity: Guiding time series forecasting with textual cues. *arXiv preprint arXiv:2405.13522*,
 607 2024.

608 Hao Xue and Flora D Salim. Promptcast: A new prompt-based learning paradigm for time series
 609 forecasting. *IEEE Transactions on Knowledge and Data Engineering*, 2023.

610

611 Jiahui Yu, Zirui Wang, Vijay Vasudevan, Legg Yeung, Mojtaba Seyedhosseini, and Yonghui
 612 Wu. Coca: Contrastive captioners are image-text foundation models. *arXiv preprint*
 613 *arXiv:2205.01917*, 2022.

614

615 Ailing Zeng, Muxi Chen, Lei Zhang, and Qiang Xu. Are transformers effective for time series
 616 forecasting? In *Proceedings of the AAAI conference on artificial intelligence*, volume 37, pp.
 11121–11128, 2023.

617

618 Yunhao Zhang and Junchi Yan. Crossformer: Transformer utilizing cross-dimension dependency
 619 for multivariate time series forecasting. In *The eleventh international conference on learning*
 620 *representations*, 2023.

621

622 Yunkai Zhang, Yawen Zhang, Ming Zheng, Kezhen Chen, Chongyang Gao, Ruian Ge, Siyuan
 623 Teng, Amine Jelloul, Jinmeng Rao, Xiaoyuan Guo, Chiang-Wei Fang, Zeyu Zheng, and Jie
 624 Yang. Insight miner: A large-scale multimodal model for insight mining from time series. In
 625 *NeurIPS 2023 AI for Science Workshop*, 2023. URL <https://openreview.net/forum?id=E1khscdUdH>.

626

627 Tian Zhou, Ziqing Ma, Qingsong Wen, Xue Wang, Liang Sun, and Rong Jin. Fedformer: Frequency
 628 enhanced decomposed transformer for long-term series forecasting. In *International conference*
 629 *on machine learning*, pp. 27268–27286. PMLR, 2022.

630

631 Tian Zhou, Peisong Niu, Xue Wang, Liang Sun, and Rong Jin. One Fits All: Power general time
 632 series analysis by pretrained lm. In *NeurIPS*, 2023.

633

634

635

636

637

638

639

640

641

642

643

644

645

646

647

648 A CROSS-MODALITY ALIGNMENT EFFICIENCY
649
650651 Table 5: Efficiency analysis of Dual-Forecaster on synthetic dataset and ETTm2.
652

Dataset-Prediction Horizon	synthetic dataset-30				ETTm2-96				
	Metric	Trainable Param. (M)	Non-trainable Param. (M)	Mem. (MiB)	Speed(s/iter)	Trainable Param. (M)	Non-trainable Param. (M)	Mem. (MiB)	Speed(s/iter)
w/ Texts		13.5	82.1	1840	0.043	13.6	82.1	8812	0.242
w/o Texts		6.5	0	672	0.022	6.6	0	928	0.036

653 B BROADER IMPACTS
654
655

656 This work introduces a groundbreaking exploration in time series forecasting—a multimodal time
657 series forecasting model that leverages textual modality data to enhance predictive capabilities for
658 time-series analysis. The broader impact of this research is multifaceted. By delivering high-fidelity
659 and reliable forecasts, it empowers advanced decision-making in critical domains such as finance and
660 healthcare, where precision is paramount. Moreover, its strong interpretability enables actionable
661 insights for optimized resource allocation and enhanced patient care protocols. The societal impli-
662 cations are profound: this work establishes a novel framework for integrating complex time-series
663 data with emerging AI technologies (e.g., LLMs), fundamentally transforming how time-series data
664 is analyzed and utilized across diverse sectors. By bridging textual semantics and temporal dynamics,
665 this approach paves the way for next-generation predictive models that address the growing
666 demand for multimodal intelligence in real-world applications.

667 C EXPERIMENTAL DETAILS
668669 C.1 IMPLEMENTATION
670

671 All the experiments are repeated three times with different seeds and we report the averaged results.
672 Our model implementation is on Pytorch (Paszke et al., 2019) with all experiments conducted on a
673 single NVIDIA GeForce RTX 4070 Ti GPU. Our detailed model configurations are in Table 6.

674 C.2 MULTIMODAL TIME SERIES BENCHMARK DATASETS CONSTRUCTION
675

676 In the realm of time series forecasting, there is a notable lack of high-quality multimodal time series
677 benchmark datasets that combine time series data with corresponding textual series. While some
678 studies have introduced multimodal benchmark datasets (Liu et al., 2024a; Xu et al., 2024), these
679 datasets primarily rely on textual descriptions derived from external sources like news reports or
680 background information. These types of textual data are often domain-specific and may not be con-
681 sistently available across different time series domains, limiting their utility for building unified mul-
682 timodal models. In contrast, shape-based textual descriptions of time series patterns are relatively
683 easier to generate and can provide more structured insights. The TS-Insights dataset Zhang et al.
684 (2023) pairs time series data with shape-based textual descriptions. However, these descriptions are
685 based on detrended series (with seasonality removed), which may introduce bias and complicate
686 the interpretation of the original time series data. To address these challenges, we propose six new
687 multimodal time series benchmark datasets where textual descriptions are directly aligned with the
688 observed patterns in the time series. The construction process for these datasets is outlined below.

689 C.2.1 SYNTHETIC DATASET
690

691 For the synthetic time series data, we firstly design three categories of components, which are then
692 combined to generate simulated time series. The components are as follows:

- 693 • **Trend:** Linear trend, exponential trend
- 694 • **Seasonality:** Cosine, linear, exponential, M-shape, trapezoidal
- 695 • **Noise:** Gaussian noise with varying variances

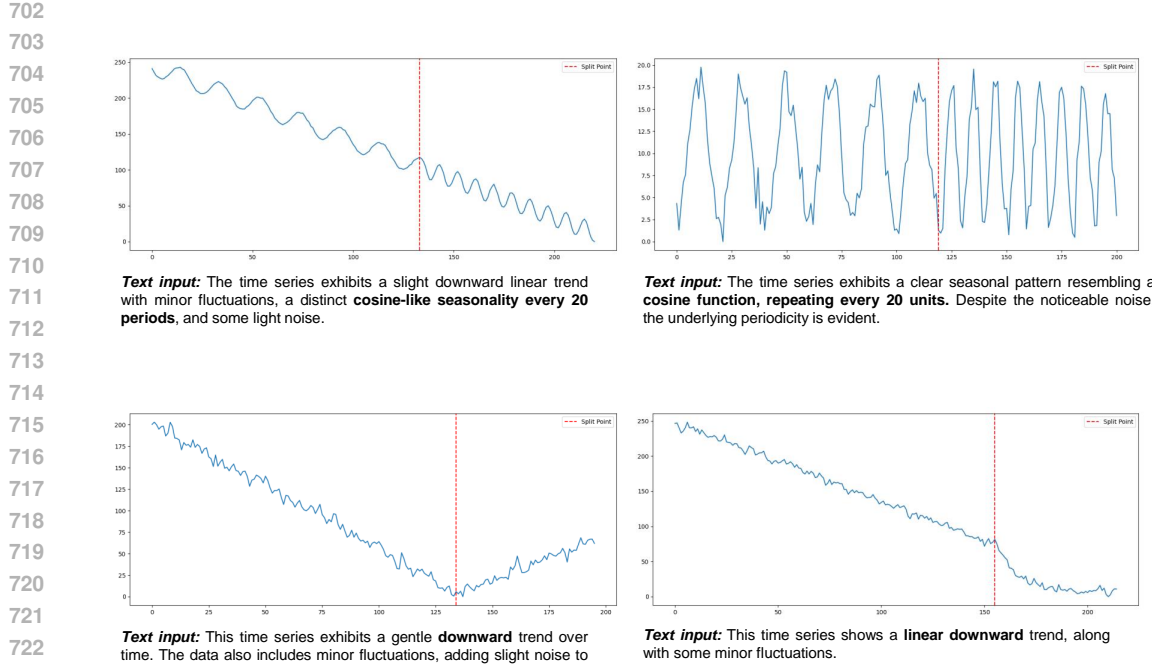


Figure 3: Synthetic time series and its paired text examples.

To generate the synthetic time series, one component from each category is randomly selected. These components are then either added together or multiplied to produce a time series, along with a corresponding textual description of its key characteristics. To enhance the diversity of the descriptions, rule-based descriptions are paraphrased using GPT-4o. Additionally, to simulate transitions between different states, we generate time series where only one component changes over time. For instance, a time series might exhibit a linear upward trend that transits to a linear downward trend. In this manner, we construct the synthetic dataset with a total of 3,040 training samples. Each sample includes time series and its paired textual series. Several examples of these constructed samples are shown in Figure 3.

C.2.2 CAPTIONED PUBLIC DATASETS

For the real-world time series data, we construct corresponding textual descriptions using the following method, and Figure 4 shows the whole caption process.

- First, we apply the Iterative End Point Fitting (IEPF) algorithm (Douglas & Peucker, 1973) to the min-max normalized time series, identifying reasonable segmentation points. IEPF begins by taking the starting curve, which consists of an ordered set of points, and an allowable distance threshold. Initially, the first and last points of the curve are marked as essential. The algorithm then iteratively identifies the point farthest from the line segment connecting these endpoints. If the distance of this point exceeds threshold, it is retained as a segmentation point, and the process is recursively repeated for the subsegments until no points are found that are farther than threshold from their respective line segments. This iterative approach ensures that the segmentation preserves the curve’s critical structure while discarding unnecessary details. The lines connecting these segmentation points can roughly outline the overall shape of the time series.
- Once the time series is segmented, statistical features such as slope and volatility are computed for each section. For each segment, a linear regression model is fitted to the data, and the slope is calculated. The P-value from the regression determines the significance of the trend: if it’s below 0.05, the slope indicates an upward or downward trend; if it’s above 0.05, the segment is considered to be fluctuating. The Mean Squared Error (MSE) between

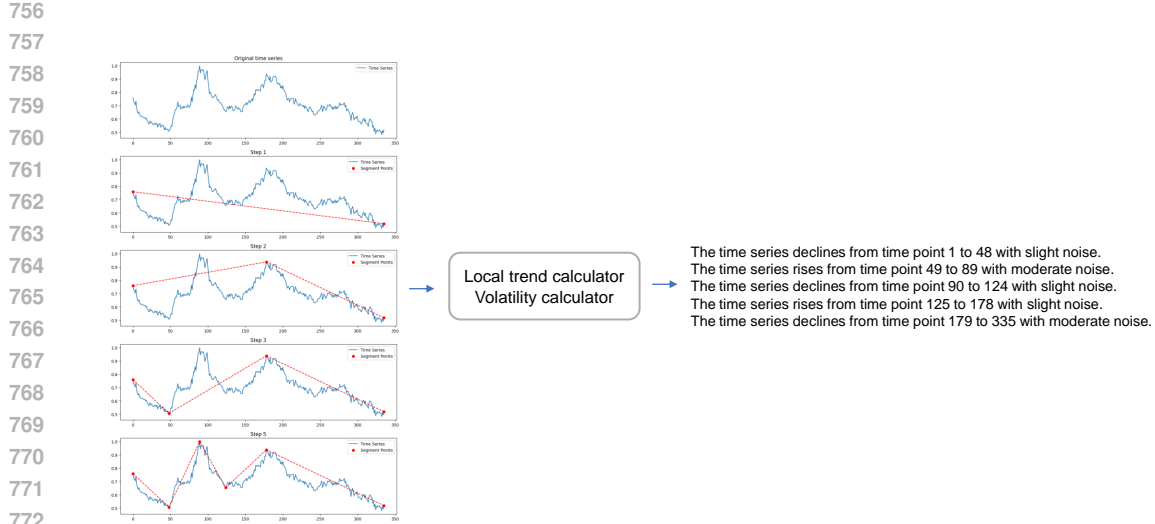


Figure 4: Captioning process for real-world time series. First, IEPF is used to segment time series, identifying reasonable segmentation points. This algorithm works by iteratively fitting straight lines between endpoints and adjusting segmentation points to minimize fitting errors, thereby identifying rational breakpoints. Next, statistical features such as slope and volatility are calculated for each segmented portion of the time series. Finally, based on these statistical characteristics, a descriptive textual summary is generated.

the original data and the regression line is also calculated to measure the noise level. Based on the MSE, the noise is classified into three levels: low, medium, or high.

- Finally, a textual description is generated: if the local trend is significant, the description notes whether the segment is increasing or decreasing; if not, it indicates fluctuation. The noise level is also included in the description based on the MSE.

We apply the above method to annotate five commonly used real-world datasets: ETTm1, ETTm2, ETTh1, ETTh2, and exchange-rate. Each dataset is divided into training and testing sets with a ratio of 8:2. Following the configurations of a look-back window of 336 and a forecasting horizon of 96, we construct training samples using a sliding window approach. Figure 5 illustrates the text annotation results on the exchange-rate dataset. Our annotation method accurately captures segmentation points (red lines), thereby producing meaningful summary shape descriptions.

It should be noted that due to resource constraints, we construct relatively small datasets on the basis of these datasets by setting the value of stride and conduct experiments on them. For ETTm1 and ETTm2 datasets, stride is set to 16, while for ETTh1 and ETTh2 datasets, stride is fixed as 4. For exchange-rate datasets, stride is set to 12.

C.3 MULTIMODAL TIME SERIES BENCHMARK DATASETS COLLECTION

Apart from our constructed multimodal time series datasets, including the synthetic dataset and captioned-public datasets, we also collect the Time-MMD dataset. The Time-MMD dataset (Liu et al., 2024a) encompasses such nine primary data domains as climate, health, energy, and traffic. It is the first high-quality and multi-domain, multimodal time series dataset, providing great convenience for verifying the model’s multimodal time series forecasting ability in real-world scenarios.

C.4 MODEL CONFIGURATIONS

The configurations of our models, in relation to the evaluations on various datasets, are consolidated in Table 6. By default, optimization is achieved through the Adam optimizer (Kingma, 2014) with a learning rate set at 0.0001 (0.005 for the Time-MMD-Economy dataset, Time-MMD-Energy dataset and Time-MMD-Health-US dataset) and a weight decay ratio of 0.01, throughout all experiments. In

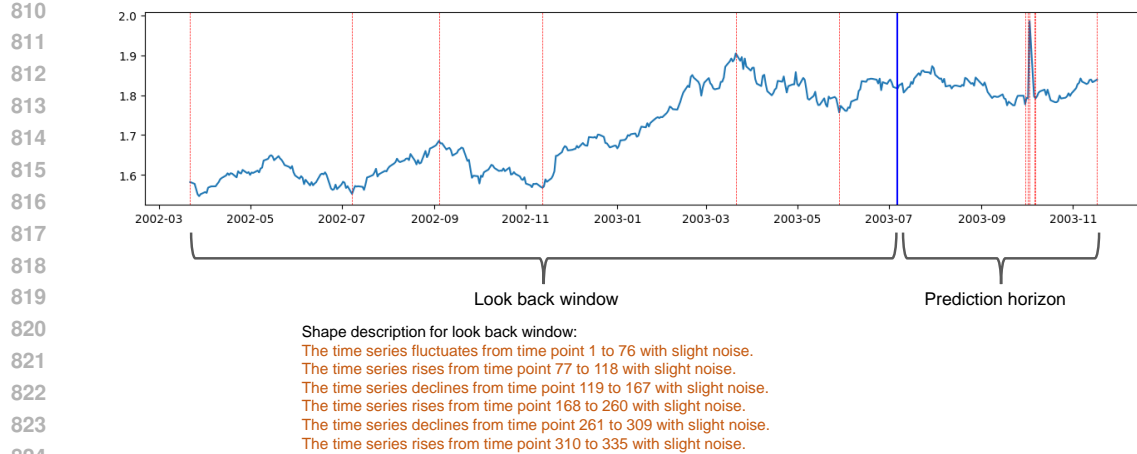


Figure 5: Visualization of a captioned example from exchange-rate dataset.

terms of dataset parameters, L and h signify the input time series *look back window* length and the future time points to be predicted, respectively. For the input time series, we firstly perform patching to obtain P non-overlapping patches with a patch length of L_p . In terms of model hyperparameters, d_m represents the dimension of the embedded representations, and n_{uni} denotes the number of layers of unimodal time series encoder used to process time series inputs, while n_{mul} denotes the number of layers of the modality interaction module, which ensures effectively alignment of distributions between historical textual and time series data. Heads are correlate to the *Multi-Head Self-Attention (MHSA)* and *Multi-Head Cross-Attention (MHCA)* operations utilized for cross-modality alignment. For the synthetic dataset and Time-MMD datasets, we set the training epochs to 300, while for the ETT, and exchange-rate datasets, we set it to 100. Additionally, to prevent overfitting, we introduce an early stopping strategy and set the patience to 7 except for the Time-MMD-Economy dataset, Time-MMD-Energy dataset and Time-MMD-Health-US dataset.

Table 6: An overview of the experimental configurations for Dual-Forecaster.

Dataset/Configuration	Dataset Parameter				Model Hyperparameter				Training Process				
	L	P	L_p	h	d_m	n_{uni}	n_{mul}	Heads	LR	Weight Decay	Batch Size	Epochs	Patience
synthetic dataset	200	25	8	30	256	6	3	8	0.0001	0.01	64	300	7
ETTm1	336	42	8	96	256	6	1	8	0.0001	0.01	64	100	7
ETTm2	336	42	8	96	256	6	3	8	0.0001	0.01	64	100	7
ETTh1	336	42	8	96	256	6	3	8	0.0001	0.01	64	100	7
ETTh2	336	42	8	96	256	6	3	8	0.0001	0.01	64	100	7
exchange-rate	336	42	8	96	256	6	3	8	0.0001	0.01	64	100	7
Time-MMD-Climate	8	1	8	8	256	2	1	4	0.0001	0.01	32	300	7
Time-MMD-Economy	8	1	8	8	64	2	1	2	0.005	0.01	32	300	20
Time-MMD-SocialGood	8	1	8	8	256	2	3	2	0.0001	0.01	32	300	7
Time-MMD-Traffic	8	1	8	8	128	2	1	4	0.0001	0.01	32	300	7
Time-MMD-Energy	40	5	8	12	128	2	1	2	0.005	0.01	32	300	20
Time-MMD-Health-US	40	5	8	12	128	2	1	2	0.005	0.01	32	300	20

864 C.5 EVALUATION METRIC
865866 We adopt the Mean Square Error (MSE) and Mean Absolute Error (MAE) as the default evaluation
867 metrics. The calculations of these metrics are as follows:
868

869
$$870 \quad MSE = \frac{1}{H} \sum_{h=1}^H (Y_h - \hat{Y}_h)^2$$

871

872
$$873 \quad MAE = \frac{1}{H} \sum_{h=1}^H |Y_h - \hat{Y}_h|$$

874

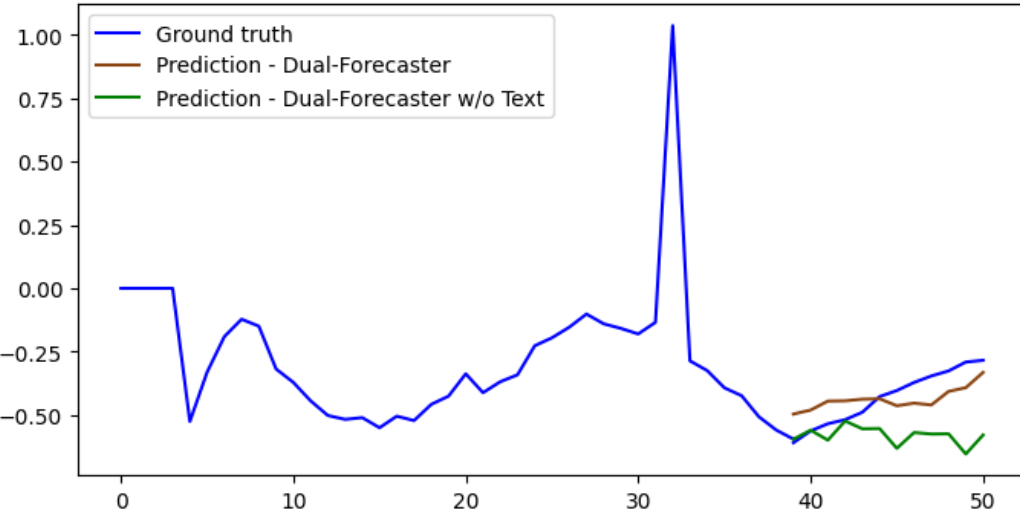
875 where H denotes the length of prediction horizon. Y_h and \hat{Y}_h are the h -th ground truth and prediction
876 where $h \in \{1, \dots, H\}$.
877880 D BASELINES
881882 **DLinear:** is a combination of a decomposition scheme and a linear network that first divides a time
883 series data into two components of trend and remainder, and then performs forecasting to the two
884 series respectively with two one-layer linear model.
885886 **FITS:** consists of the key part of the complex-valued linear layer that is dedicatedly designed to
887 learn amplitude scaling and phase shifting, thereby facilitating to extend time series segment by
888 interpolating the frequency representation.
889890 **PatchTST:** is composed of two key components: (i) patching that segments time series into patches
891 as input tokens to Transformer; (ii) channel-independent structure where each channel univariate
892 time series shares the same Transformer backbone.
893894 **iTransformer:** is an inverted Transformer that raw series of different variates are firstly embedded
895 to tokens, applied by self-attention for multivariate correlations, and individually processed by the
896 share feed-forward network for series representations of each token.
897898 **Chronos:** is a framework that adapts language model architectures and training procedures to prob-
899 abilistic time series forecasting by tokenizing time series values into a fixed vocabulary.
900901 **GPT4TS:** is a unified framework that uses a frozen pre-trained GPT2 for general time series anal-
902 ysis tasks including time series classification, short/long-term forecasting, imputation, anomaly de-
903 tection, few-shot and zero-sample forecasting.
904905 **UniTime:** is a unified model for cross-domain time series forecasting. It overcomes challenges
906 like varying data characteristics, domain confusion, and convergence speed imbalance, and shows
907 superior performance and zero-shot transferability through experiments on multiple datasets.
908909 **Time-LLM:** is a new framework, which encompasses reprogramming time series data into text
910 prototype representations before feeding it into the frozen LLM and providing input context with
911 declarative prompts via Prompt-as-Prefix to augment reasoning.
912913 **MM-TSFlib:** is the first multimodal time-series forecasting (TSF) library, which allows the integra-
914 tion of any open-source language models with arbitrary TSF models, thereby enabling multimodal
915 TSF tasks based on Time-MMD.
916917 **TimeCMA:** is an LLM-empowered framework for multivariate time series forecasting. It addresses
918 data entanglement issues by using a dual-modality encoding and cross-modality alignment, and
919 reduces computational costs through last token embedding storage.
920921 **ChatTime:** is a multimodal time series foundation model that treats time series as a foreign lan-
922 guage. It provides zero-shot capability and supports bimodal input/output for both time series and
923 text.
924

918 E ERROR BARS
919

920 All experiments are repeated three times except for ChatTime and Chronos, which execute only
921 one inference. The comparison between our method and all the baseline methods on all datasets is
922 delineated in Table 7.

924 Table 7: Standard deviations of Dual-Forecaster and baseline models across all datasets (MSE re-
925 ported).

Model	Dual-Forecaster	GPT4TS	UniTime	Time-LLM	MM-TSFlib	TimeCMA	ChatTime	Chronos	DLinear	FITS	PatchTST	iTransformer
Dataset	MSE	MSE	MSE	MSE	MSE	MSE	MSE	MSE	MSE	MSE	MSE	MSE
synthetic dataset	0.5970±0.0182	0.9467±0.0570	0.6684±0.0241	0.8907±0.0296	0.6013±0.0020	3.0644±0.0132	1.1251	0.9273	1.2190±0.0254	2.7585±0.3402	0.6015±0.0063	0.6190±0.0061
ETTm1	1.3203±0.0138	1.4641±0.0303	1.4034±0.0165	1.4457±0.0048	1.3620±0.0085	2.4790±0.0013	1.7347	1.5638	1.5601±0.0106	2.2858±0.1409	1.4544±0.0348	1.3393±0.0045
ETTm2	0.9363±0.0069	1.1184±0.0351	1.0397±0.0156	1.1199±0.0375	1.0325±0.0157	2.0336±0.0021	1.8680	1.6991	1.1663±0.0069	1.7418±0.0415	0.9419±0.0400	1.0210±0.0123
ETTth1	1.3955±0.0353	1.5078±0.0949	1.4647±0.0255	1.5919±0.1427	1.4967±0.0333	1.6117±0.0042	1.9604	1.5282	1.4999±0.0043	1.6004±0.0335	1.6009±0.0840	1.5128±0.0146
ETTth2	0.9429±0.0332	0.9612±0.0183	1.0028±0.0312	1.0586±0.1008	0.9616±0.0080	1.4177±0.0070	1.5014	1.0474	0.9951±0.0015	1.2858±0.0306	1.0349±0.0578	0.9903±0.0292
exchange-rate	2.2011±0.0161	3.0947±0.1516	2.5676±0.3719	3.0564±0.0877	2.6365±0.0959	4.4906±0.0213	2.3079	2.7269	3.1668±0.0148	4.4656±0.2718	2.2656±0.0460	2.6426±0.0141
Time-MMD-Climate	0.8520±0.0018	0.14222±0.0491	1.2687±0.0841	1.3398±0.0845	1.1386±0.0612	1.3713±0.0139	1.5118	1.0344	2.9057±0.3899	1.5498±0.0868	1.0975±0.0130	1.1392±0.0186
Time-MMD-Economy	0.1785±0.0038	0.2350±0.0063	0.2691±0.0111	0.2310±0.0066	0.2066±0.0051	0.2234±0.0005	0.3199	0.2782	8.1634±1.7173	0.2766±0.0340	0.1960±0.0029	0.1963±0.0037
Time-MMD-SocialGood	1.2364±0.0310	1.5420±0.0254	1.8239±0.2461	1.5172±0.0413	1.8615±0.0280	1.5433±0.0033	1.6290	1.5912	4.3273±0.6212	1.7227±0.1214	1.7509±0.1066	1.7128±0.5985
Time-MMD-Traffic	0.1814±0.0010	0.2763±0.0031	0.3127±0.0418	0.2299±0.0335	0.1892±0.0076	0.2805±0.0005	0.4648	0.3920	4.3517±1.0442	0.3542±0.0761	0.1828±0.0026	0.1917±0.0017
Time-MMD-Energy	0.0853±0.0044	0.2069±0.0391	0.1158±0.0018	0.1263±0.0223	0.1146±0.0027	0.2553±0.0025	0.5051	0.1193	1.2069±0.1884	0.2893±0.0524	0.1031±0.0058	0.1123±0.0029
Time-MMD-Health-US	0.8563±0.0287	1.5428±0.1567	1.0753±0.0176	1.1728±0.0290	0.9710±0.1153	2.0369±0.0051	1.5114	1.5394	2.2140±0.2037	2.2509±0.2076	1.1000±0.0299	1.0467±0.0217



954 Figure 6: **Case study about interpretability of textual influence from Time-MMD-Health-US.**